Electronic Supplementary Information (ESI)

Designing a Carbon-Encapsulated $ZnS/SnS_2/SnO_2$ Heterojunction Secondary Battery Anode Displaying Large Capacity and Good Stability

Jinyun Liu[a,*], Yongmei Hua[a], Huizi Songtian[a], Shenglan Li[a], Yin Peng[a,*], Zeng Pan[b,*]

[a.] Key Laboratory of Functional Molecular Solids, Ministry of Education, College of Chemistry and Materials Science, Anhui Normal University, Wuhu, Anhui 241002, PR China

[b.] Shenzhen BYD Lithium Battery Co., Ltd., Shenzhen, Guangdong 518116, PR China

[*] Corresponding Author.

Jinyun Liu (jyliu@iim.ac.cn), Yin Peng (kimipeng@mail.ahnu.edu.cn); Zeng Pan (zengpan@nankai.edu.cn).

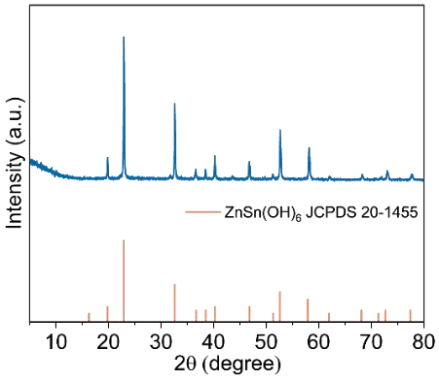

Fig. S1 XRD pattern of the $ZnSn(OH)_6$ precursor.

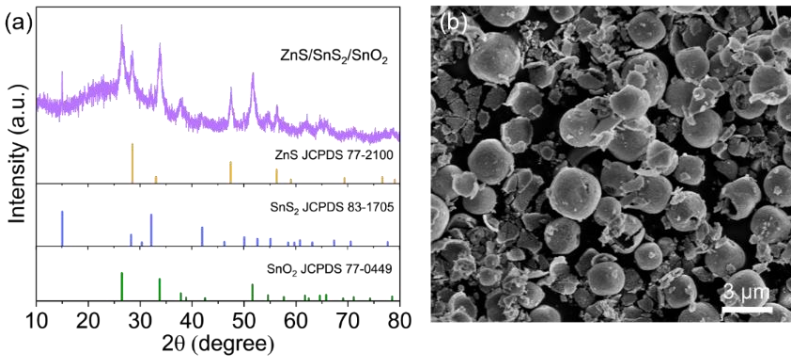

Fig. S2 (a) XRD pattern and (b) SEM image of $ZnS/SnS_2/SnO_2$.

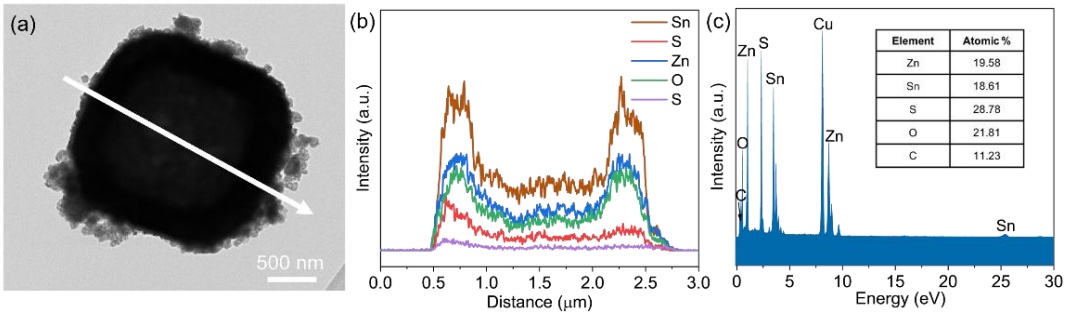

Fig. S3 (a) SEM image, (b) line-scanning curves, and (c) EDS spectrum of $ZnS/SnS_2/SnO_2$@C.

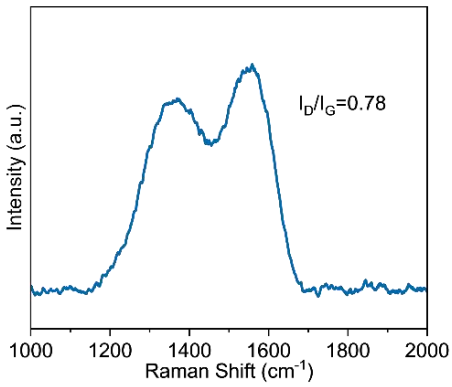

Fig. S4 Raman spectrum of $ZnS/SnS_2/SnO_2$@C.

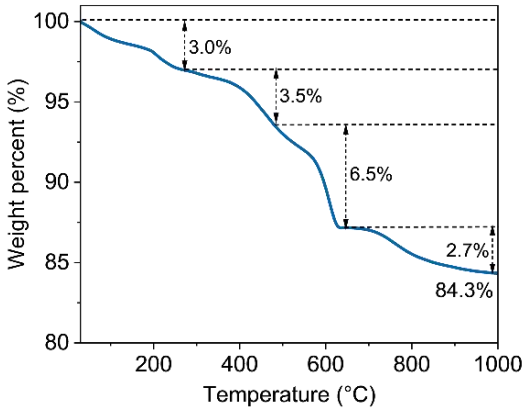

Fig. S5 TGA curve of $ZnS/SnS_2/SnO_2$@C.

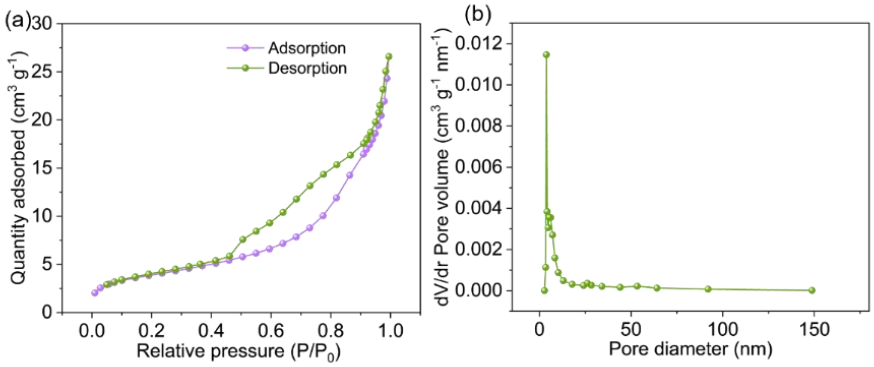

Fig. S6 (a) N_2 adsorption-desorption isotherms and (b) pore-size distribution of $ZnS/SnS_2/SnO_2$@C.

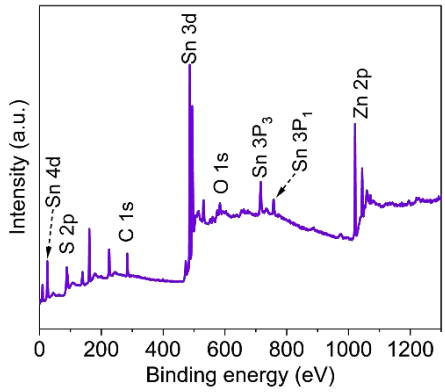

Fig. S7 XPS survey spectrum of $ZnS/SnS_2/SnO_2$@C.

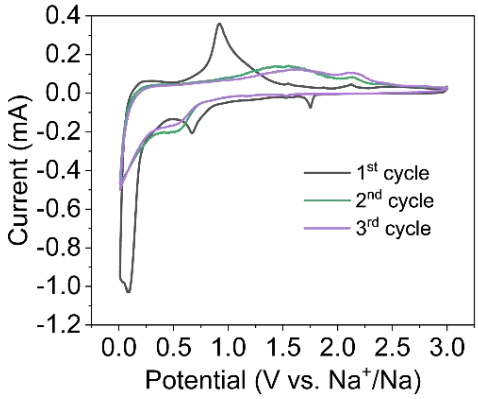

Fig. S8 CV curves of $ZnS/SnS_2/SnO_2$ during the initial three cycles at 0.1 mV s^{-1}.

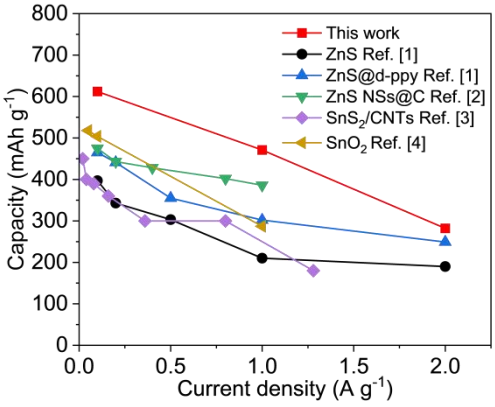

Fig. S9 Comparison on the performance of the $ZnS/SnS_2/SnO_2$@C with some ZnS, SnS_2, or SnO_2-based anodes.

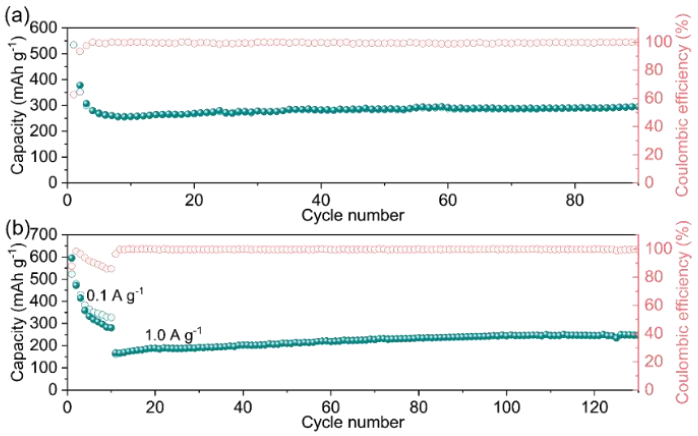

Fig. S10 Cycling performance of $ZnS/SnS_2/SnO_2$@C under -10 °C at (a) 0.5 and (b) 1.0 A g^{-1}. In (b), the anode was pre-activated 10 times at 0.1 A g^{-1}.

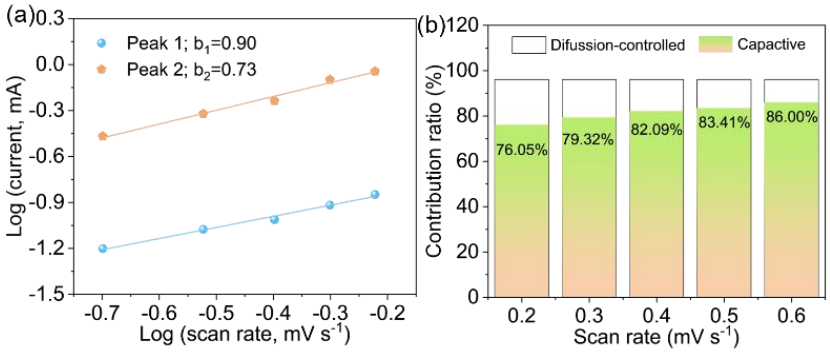

Fig. S11 (a) The log(*i*) versus log(*v*) plots for oxidization and reduction, and (b) the contribution of capacitive and diffusion-controlled processes of $ZnS/SnS_2/SnO_2$@C.

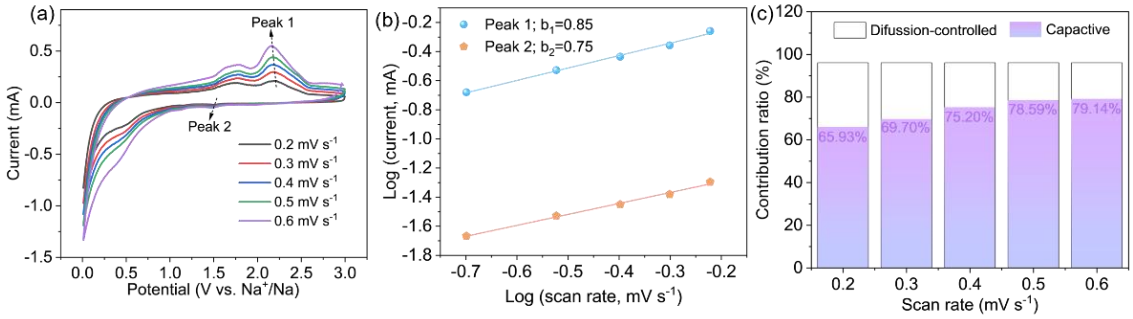

Fig. S12 (a) CV curve of $ZnS/SnS_2/SnO_2$ anode at scanning rates from 0.2 to 0.6 mV s^{-1}. (b) The log(i) vs. log(v) of oxidization and reduction peaks. (c) Contribution ratio of capacitive and diffusion-control processes.

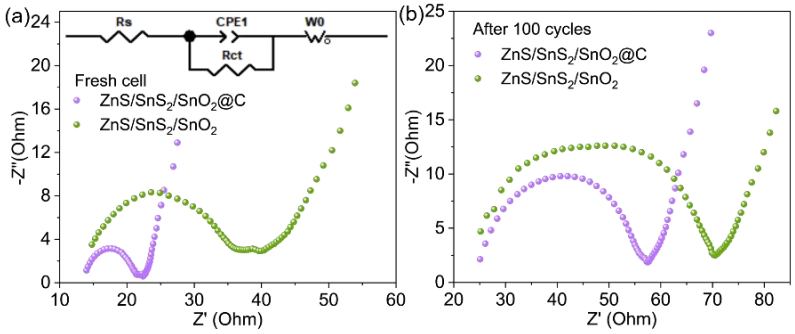

Fig. 13 EIS spectra of $ZnS/SnS_2/SnO_2$@C and $ZnS/SnS_2/SnO_2$ (a) before and (b) after 100 cycles at 1.0 A g^{-1}.

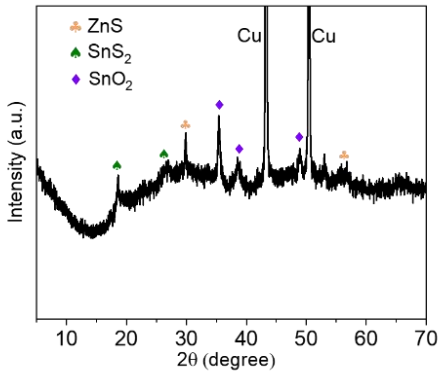

Fig. S14 XRD pattern of $ZnS/SnS_2/SnO_2$@C after cycling 100 times at 1.0 A g^{-1}.

Table S1. Bond distances and coordination numbers for $ZnS/SnS_2/SnO_2$@C. Information obtained from EXAFS K and R space transformations with fitting. The low R factors confirm the quality of the fitting.

samples	path	C.N.[a]/N	R (Å)[b]	σ^2 (x 10^{-3} Å^2)[c]	R−factor[d]
$ZnS/SnS_2/SnO_2$@C	Zn-S	1.0	2.34	3.70	0.023

[a] Coordination number.

[b] Bond distance.

[c] Debye−Waller factor.

[d] Sum of squares measure of the fractional misfit.

The accuracies of the above parameters were estimated as CN, ±20%; R, ±1%; σ^2, ±20%.

Table S2. Comparison on electrochemical performance of Na-ion battery anodes.

Anode materials	Mass loading (mg cm^{-2})	Current density (A g^{-1})	Capacity (mAh g^{-1})	Cycle number	Ref.
$ZnS/SnS_2/SnO_2$@C	1.2	0.1	612	100	This study
		1.0	471	400	
UltraPhene™/s-SnS_2	1.0-2.0	0.1	308	100	[5]
SnS-SnS_2@CNTs	1.0-1.5	0.1	413	50	[6]
Few-layered MoS_2@SnO_2@C	1.0-1.5	0.1	415	50	[7]
Sb/SnO_2@C	1.1	1.0	115	2000	[8]
Porous carbon/C@SnO_2@$BaTiO_3$	1.0-1.5	0.1	372	300	[9]
FeS/ZnS	1.5	0.1	475	50	[10]
ZnS-Sb@C@rGO	1.2-1.5	1.0	210	300	[11]
NiS/ZnS@C	1.1	1.0	414	180	[12]

References

1 T. Y. Hou, G. J. Tang, X. H. Sun, S. Cai, C. M. Zheng and W. B. Hu, RSC Adv., 2017, 7, 43636-43641.

2 W. Ji, L. Hu, X. Hu, Y. C. Ding and Z. H. Wen, Mater. Today Commun., 2019, 19, 396-401.

3 Y. R. Ren, J. W. Wang, X. B. Huang and J. N. Ding, Mater. Lett., 2017, 186, 57-61.

4 H. Y. Li, X. T. Jia, B. Huang, J. W. Yang, Y. W. Li and S. K. Zhong, Nanotechnology, 2023, 325602.

5 P. C. Tai, R. J. Chung, C. Kongvarhodom, S. Husain, S. Yougbaré, H. M. Chen, Y. F. Wu and L. Y. Lin, *J. Colloid Interface Sci.*, 2024, **679**, 691–702.

6 Q. Li, S. R. Wang, Y. Wang, H. Z. Ma, J. J. Du, X. H. He, N. Huang, C. L. Li, W. P. Wang and Y. Q. Weng, *Mater. Lett.*, 2024, **366**, 136476.

7 Z. L. Wu, Z. Q. Huang, M. X. Yu, Y. N. Du, J. W. Li, H. Jia, Z. Y. Lin, X. H. Huang and S. M. Ying, *Dalton Trans.*, 2024, **53**, 15920-15927.

8 J. A. Wu, C. L. Liu, H. B. Huang, M. L. Xie, D. Ma and X. Liang, *J. Electroanal. Chem.*, 2024, **978**, 118888.

9 M. C. Ye, J. M. Ye, Z. Y. Zhang, Z. Y. Feng, D. P. Xiong and M. He, *J. Power Sources*, 2025, **630**, 236160.

10 D. L. Xie, S. Cai, X. H. Sun, T. Y. Hou, K. E. Shen, R. Ling, A. R. Fan, R. Z. Zhang, S. Jiang and Y. S. Lin, *Inorg. Chem. Commun.*, 2019, **111**, 107635.

11 M. Zhu, Y. Jiang, X. J. Yang, X. S. Li, L. Y. Wang and W. Lü, *ACS Appl. Nano Mater.*, 2023, **6**, 13503-13512.

12 J. J. Wang, J. X. Fan, M. Y. Fan, X. Y. Yue, J. Zhang, Z. Liu, Z. K. Xie, Q. Zhao, A. Abudula and G. Q. Guan, *J. Power Sources*, 2024, **626**, 235803.